Brazilian Journal of Medical and Biological Research (2025) 58: e14408, https://doi.org/10.1590/1414-431X2025e14408
ISSN 1414-431X Research Article

Low-intensity pulsed ultrasound inhibits chondrocyte senescence by inhibiting PI3K/AKT/mTOR signaling

Wang Han[1,2], Mengtong Guan[1], Bo Liao[1], Xiaoyu Han[1], Kaiting Li[1], Qing Chen[1], Xiya Guo[1], Yajuan Niu[1], Ying Zhu[1]✉, and Dingqun Bai[1]✉

[1]Department of Rehabilitation Medicine, The First Affiliated Hospital of Chongqing Medical University, Chongqing, China
[2]The Chongqing Key Laboratory of Translational Medicine in Major Metabolic Diseases, The First Affiliated Hospital of Chongqing Medical University, Chongqing, China

Abstract

Cellular senescence is an important cause of age-related degenerative diseases, including osteoarthritis (OA). Chondrocyte senescence is crucial in OA onset and progression. As a non-invasive, safe, and widely used physical rehabilitation factor, the effect and mechanism of low intensity pulsed ultrasound (LIPUS) on chondrocyte senescence remain unclear. This study evaluated the inhibitory effect of LIPUS on OA chondrocyte senescence *in vitro* and *in vivo*. The effect of LIPUS on chondrocyte senescence was examined by RT-qPCR, enzyme-linked immunosorbent assay (ELISA), and western blotting. Changes in levels of reactive oxygen species (ROS) and γ-h2ax foci in senescent chondrocytes were detected using fluorescent staining. Chondrocyte senescence was evaluated by senescence-associated β-galactosidase (SA-β-gal) staining. The PI3K inhibitor LY294002 and the PI3K agonist 740Y-P were used to investigate whether PI3K/AKT/mTOR signalling was involved in the effect of LIPUS in senescent chondrocytes. Chondrocyte senescence and cartilage degeneration were analyzed in a destabilization of the medial meniscal (DMM) mouse model by immunohistochemistry, hematoxylin and eosin staining, and safranin-O/fast green staining. LIPUS inhibited the expression of the senescence-associated secretory phenotype (SASP) factors CCL4 and CCL2 and the senescence phenotype in doxorubicin-treated chondrocytes by inhibiting the PI3K/AKT/mTOR pathway. LIPUS alleviated chondrocyte senescence and attenuated OA progression in the DMM mice. These results demonstrated a novel role for LIPUS in inhibiting chondrocyte senescence and the SASP by modulating PI3K/AKT/mTOR signalling. Our findings expanded the clinical application of LIPUS and provide a new, non-invasive, and safe treatment approach to prevent and treat age-related degenerative joint disorders.

Key words: Cellular senescence; Chondrocytes; Osteoarthritis; Ultrasonic waves

Introduction

Cellular senescence is a stress response that triggers a permanent cell cycle arrest and causes significant phenotypic alterations, such as the release of damaging pro-inflammatory chemicals into the surrounding micro-environment, which is termed senescence-associated secretory phenotype (SASP) (1). Stimuli such as oxidative stress, chronic inflammation, and aberrant mechanical stress all contribute to chondrocyte senescence (2). The cellular senescence program is initiated by the $p16^{INK4a}$/Rb and/or p53/p21CIP1 tumor suppressor pathways (3). Cell senescence not only leads to aging, but also causes many age-related diseases.

Lingering senescent cells drive age-related diseases such as osteoarthritis (OA). OA is the most prevalent chronic joint disease and is characterized by gradual deterioration of articular cartilage (4). Senescence is considered an integral driver of cartilage degeneration in OA (5). Senescent chondrocytes might contribute to cartilage degeneration by releasing pro-inflammatory mediators, which include cytokines, chemokines, and matrix-degrading molecules known as SASP (6). Several studies have reported that PI3K/AKT/mTOR signaling is crucial to maintaining cartilage homeostasis. Recent studies reported that drugs prevent OA chondrocyte senescence by inhibiting the PI3K/AKT/mTOR signaling pathway (7). Another study revealed that chondrocyte clearance attenuated post-traumatic OA development and promoted cartilage homeostasis (8). Accordingly, targeting chondrocyte senescence might present a novel approach to prevent cartilage degeneration and attenuate OA progression.

As a non-invasive and safe physical therapy, low intensity pulsed ultrasound (LIPUS) has been proven to have anti-inflammatory, pro-repair, and neuromodulatory

Correspondence: Ying Zhu: <yingzhu517@hospital.cqmu.edu.cn> | Dingqun Bai: <baidingqun@hospital.cqmu.edu.cn>

Received October 24, 2024 | *Accepted January 25, 2025*

characteristics (9). Furthermore, recent research shows that LIPUS exhibits some efficacy in inhibiting senescence. LIPUS attenuates human testicular Leydig cell senescence in culture (10). Moreover, LIPUS delayed chronic kidney disease progression *in vivo* by regulating senescent markers (11).

Previous studies have shown that LIPUS might affect various pathophysiological processes by regulating PI3K/AKT/mTOR signaling. A study conducted by Zhou et al. (12) suggests that LIPUS may promote autophagy and inhibit apoptosis by inhibiting PI3K/AKT/mTOR signaling to alleviate premature ovarian failure (POF). Another interesting study demonstrates that LIPUS induced the modulation of autophagy in lung cancer cells through the activation or inactivation of AKT/mTOR signaling, consequently influencing the release of exosomes in lung cancer cells (13). Nevertheless, the effect and mechanism of LIPUS on chondrocyte senescence in OA remain unclear.

This study investigated the effects of LIPUS in OA chondrocyte senescence *in vitro* and *in vivo*. A doxorubicin (DOX)-induced senescent chondrocyte model and a destabilization of the medial meniscal (DMM) mouse model were constructed. Chondrocyte senescence, intracellular reactive oxygen species (ROS) levels, SASP factor expression, and PI3K/AKT/mTOR signaling were assessed *in vitro*. Additionally, the effect of LIPUS on inhibiting the OA chondrocyte senescence was evaluated *in vivo*.

Material and Methods

Reagents

Doxorubicin hydrochloride (98%) was purchased from Aladdin (China). Streptomycin-penicillin solution, collagenase type II and pancreatin, F12/DMEM medium, and fetal bovine serum (FBS) were provided by Gibco (USA). PI3K inhibitor LY294002 and PI3K agonist 740 YP were acquired from MCE (USA). The senescence β-galactosidase staining kit, bicinchoninic acid assay (BCA) kit, RIPA lysis buffer, Hoechst staining kit, and a ROS assay kit were provided by Beyotime Biotechnology (China). Rat/mouse cxcl-1 ELISA kit and mouse ccl4 ELISA kit were provided by Enzyme-linked Biotechnology (China). Mouse CCL4 ELISA kit was obtained from Elabscience Biotechnology (China). Mouse/Rat CCL2 ELISA kit and Rat MMP-13 ELISA kit were purchased from Elabscience Biotechnology. Accurate Biotechnology (China) provided the kits for the qPCR reactions. The antibodies for p21, γh2ax, collagen II, MMP-13, and β-actin were provided by Abcam (UK). The antibodies for PI3K/pPI3K, AKT/pAKT, and mTOR/PmTOR were provided by Cell Signaling Technology (USA). Anti-p16ink4a antibodies were provided by Santa Cruz Biotechnology (USA) and the antibodies for p53 and Lamin B1 were from Proteintech Biotechnology (China).

Harvest and culture of chondrocytes

Rat chondrosarcoma (RCS) cells are stable differentiated chondrocytes, and were donated by the State Key Laboratory of Trauma, Burns and Combined Injury, Daping Hospital, Army Medical University (China). Primary chondrocytes were harvested from the articular cartilage of both knees of five-day-old C57BL/6 mice. After the knee joint was separated, it was digested with 0.25% trypsin for 15 min, and then the cartilage particles were separated under a stereomicroscope (PXS-D, Shanghai Optical Instrument Factory No. 6, China). Cartilage particles were digested in an incubator with 0.1% collagenase II at 37°C and 5% carbon dioxide for 6 h to obtain chondrocytes. The chondrocytes were then routinely cultured by DMEM/F12 medium supplemented with FBS and placed in a 37°C and 5% carbon dioxide incubator.

Senescent chondrocytes and LIPUS treatment

To induce chondrocyte senescence, we treated chondrocytes with 100 nM DOX for 5 days. For the activation and inhibition of signaling pathways, chondrocytes were pre-treated by 30 μM 740Y-P or 50 μM LY294002 for 2 h. Each LIPUS (Smith & Nephew Exogen 4000, USA) treatment of chondrocytes lasted 20 min, followed by the collection of cell samples. LIPUS treatment of chondrocytes was performed under sterile and room temperature conditions. The LIPUS probe was placed under a 3.5-cm dish or six-well plate, and a bubble-free medical coupling agent (OME-250G, Guangzhou Rainhome Pharm & Tech, China) was used to connect the two planes to ensure optimal ultrasound exposure. In our preliminary study, we compared the therapeutic effects of 30, 40, and 50 mW/cm^2 LIPUS on DOX-induced senescent chondrocytes. However, no statistically significant differences were observed among the different intensities (Supplementary Figure S1). Therefore, based on the preliminary foundation of our research group and the support of previous literature, we selected the classic FDA-certified treatment parameters of an intensity of 30 mW/cm^2, a frequency of 1.5 MHz, a repetition rate of 1 kHz, and a duty cycle of 20% for the subsequent research (14–16).

qRT-PCR

Total RNA was isolated from chondrocytes utilizing the RNA extraction kit (Accurate Biotechnology) based on the spin column method, and enzyme-free consumables were used throughout the extraction process. The extracted RNA was dissolved in enzyme-free water and placed on ice. Subsequently, RNA concentration and purity were measured utilizing NanoDrop-1000 spectrophotometer (Thermo Scientific, USA). According to instructions (Accurate Biotechnology), gDNA was removed and cDNA was synthesized by reverse transcription (20 μL reaction system, 1 μg RNA in total). The qPCR reaction was

carried out according to the instructions of SybrGreen qPCR mix Kit (Accurate Biotechnology) and the following reaction system (5 μL SybrGreen + 0.2 μL pre-primer + 0.2 μL post-primer + 3.6 μL enzyme-free water + 1 μL cDNA) on the MX3000P System (Agilent, USA) was used for the two-step amplification. The details of the primers are presented in Table 1.

ELISA

The chondrocyte culture supernatant was harvested and centrifuged (800 *g*, 4°C, for 10 min) to remove impurities such as cell debris. Following the instructions in the ELISA kit, a standard curve was constructed from gradient standard protein samples. A microplate reader (EL-450, USA) was used to detect the absorbance of the sample at a wavelength of 450 nm, and then the expression level of specific proteins was calculated in the sample based on the standard curve.

Western blotting

The treated chondrocytes were lysed by RIPA lysis buffer, which included protease inhibitors under ice-cold conditions for 25 min. The protein lysate was then harvested using a cell scraper, and cell debris was eliminated through centrifugation at 10,000 *g* for 15 min at 4°C. Protein levels were quantified by bicinchoninic acid (BCA) acid assay kit. The loading buffer (Beyotime, China) was added to the protein lysis solution, mixed, and then denatured in a water bath at 95°C for 10 min to obtain a protein sample. Protein samples in equal quantities were applied to a 4–20% SDS-PAGE gel and blotted onto a PVDF membrane (Bio-Red, USA). The membrane was blocked with 5% skim milk at 37°C for 120 min. After washing in TBST buffer, the membrane was incubated with the selected primary antibody overnight at 4°C. Following four washes of the membrane with TBST, the secondary antibody was incubated at 37°C for 1 h. After washing again with TBST, the immunoreactivity was evaluated by chemiluminescence method and photographed for recording. FusionCapt Advance Solo 4 16.08a (VIBER, France) system was used for gray value quantification of protein immunoblots. Subsequently, the expression level of the target protein was normalized by the internal reference.

Intracellular ROS detection

ROS assay kits (Beyotime) were used to detect intracellular ROS. DCFH-DA served as a fluorescent probe that could pass freely through the cell membrane to indicate ROS. According to the instructions of the kit, chondrocytes were incubated with 0.1% DCFH-DA at 37°C for 20 min. After washing with cell culture medium, the green fluorescence was visualized using a fluorescence microscope (Axio Observer A1/D1/Z1, Zeiss, Germany).

β-galactosidase staining

Senescence β-galactosidase staining kits (Beyotime Biotechnology) were used to stain chondrocytes. After four washes with PBS, the chondrocytes were fixed in the fixative solution at 37°C for 15 min. The staining solution was prepared according to the kit instructions. Finally, the fixed chondrocytes were incubated overnight at 37°C in a non-carbon dioxide incubator. The next day, the ratio of positive cells was observed and recorded under an inverted microscope (Axio Observer A1/D1/Z1, Zeiss, Germany).

Cell immunofluorescence

Chondrocytes were inoculated onto confocal petri dishes for culture. After treatment, chondrocytes were carefully washed three times with PBS buffer and subsequently fixed in 4% paraformaldehyde at 37°C for 15 min. Subsequently, the chondrocytes were permeabilized with 0.1% TritonX-100 for 10 min at 37°C. After blocking with blocking solution (P0102, Beyotime Biotechnology) at 37°C for 0.5 h, the chondrocytes were incubated with primary antibodies at 4°C for 18 h. Chondrocytes were washed gently with PBS three times and then incubated with secondary antibodies in the dark at room temperature for one hour. Finally, the nuclei were stained with Hoechst 33342 (C1029, Beyotime) at 37°C for 10 min, and then observed and recorded by laser confocal scanning microscope (LSM900, Zeiss, Germany).

Table 1. Primer sequences for RT-PCR.

Target gene	Forward primer	Reverse primer
GAPDH	GACATGCCGCCTGGAGAAAC	AGCCCAGGATGCCCTTTAGT
CCL2	CTCACCTGCTGCTACTCATTCACTG	CTTCTTTGGGACACCTGCTGCTG
CCL4	TCTGCGTGTCTGCCTTCTCTCTC	AAGTGGGAGGGTCAGAGCCTATTG
CXCL1	GCAGACAGTGGCAGGGATTCAC	TGAGTGTGGCTATGACTTCGGTTTG
CDKN1a	TCCTGGTGATGTCCGACCTGTTC	GGCTCAACTGCTCACTGTCCAC
CDKN2a	GAGGGCTTCCTAGACACTCTGGTAG	AGATACCGCAAATACCGCACGAC
IL-6	ACTTCCAGCCAGTTGCCTTCTTG	TGGTCTGTTGTGGGTGGTATCCTC
IL-17	TGCCTGATGCTGTTGCTGCTAC	GCGTTTGGACACACTGAACTTTGAG

Animal experiments

For animal experiments, the LIPUS treatment parameters were as follows: intensity of 30 mW/cm^2, frequency of 1.5 MHz, repetition rate of 1 kHz, and duty cycle of 20% (14–16). All animal experimental procedures were approved by the Ethics Committee of the First Affiliated Hospital of Chongqing Medical University (No. 2022-K173). Eight-week-old C57BL/6 male mice were obtained from the Chongqing Medical University (China). Firstly, mice were randomly and equally allocated into DMM and DMM + LIPUS group. As in our prior study, we performed the DMM surgery on the right knee of mice and a sham operation on the left knee as a control. To avoid wound infection, the LIPUS treatment (20 min/day) was scheduled on the third day following the DMM procedure. After anesthetizing the mice, the hair on the knee joint was shaved off and a coupling agent was applied. Subsequently, the mouse was placed in the prone position with its knee joint centered at the LIPUS probe, and bubble-free medical coupling agent was used to fully connect the knee joint and the probe. The mice in the DMM group were submitted to the treatment setup, but the LIPUS switch was not turned on. LIPUS treatment continued until week 4, after which the mice were euthanized.

Tissue sample preparation

Four weeks after DMM surgery, mice were sacrificed by carbon dioxide inhalation. The knee joint was harvested and fixed overnight in 4% paraformaldehyde at 4°C, then decalcified in 12.5% EDTA for two weeks, with regular solution changes every three days. The samples were then embedded in paraffin, and sagittal sections of the entire knee joint were cut at a thickness of 5 μm.

Histology

Sections were deparaffinized in xylene and dehydrated through graded ethanol (100, 95, 70%). Then, the sections were stained with fast green/safranin O (Beyotime) or hematoxylin/eosin staining solution (Beyotime) for 3–5 min. Next, the sections were washed with alcohol to remove excess dye and dehydrated again. Xylene was used to clear the sections, and finally the sections were mounted with optical resin and observed under an inverted microscope. Cartilage thickness and subchondral bone changes were assessed in accordance with the Osteoarthritis Research Society International (OARSI) guidelines. Scoring was performed by two independent researchers, both blinded to the treatment groups, to minimize bias (17). Cartilage score was used to evaluate the extent of cartilage erosion, with scores assigned on a scale from 0 (normal) to 6 (severe erosion), reflecting increasing severity of damage.

Immunohistochemistry (IHC)

Sections were dewaxed in xylene, and heat-induced antigen retrieval was performed in a citrate buffer (pH 6.0) at 95°C for 20 min. Sections were then blocked with 10% goat serum for 1 h at room temperature and incubated with the primary antibody overnight at 4°C. The antibodies used included [p21, Abcam, ab188224, 1:1000; p16ink4a, Santa Cruz, SC-1661, 1:100; p53, Abcam, ab32049, 1:50; Lamin B1, Affinity, AF5161, 1:100; Collagen II, Affinity, AF0135,1:100; MMP-13, Affinity, AF5355, 1:100], which have been validated for use in IHC. Afterward, biotinylated secondary antibody [Goat Anti-Rabbit/Mouse IgG HRP, Abcam, ab6721/ab205719, 1:1000], and horseradish peroxidase-conjugated streptavidin were applied for 1 h at room temperature. Sections were counterstained with hematoxylin, dehydrated, and cleared before mounting for microscopy.

Quantification of immunolabeled cells

Quantification of immunolabeled cells was performed using ImageJ software (NIH, USA). The number of positive cells was counted in three random fields of view per section, and results are reported as the average number of labeled cells per field. Statistical analysis was conducted to compare differences between groups.

Statistical analyses

Image-pro plus 6.0 (Media Cybernetics, USA) was adopted to calculate the number of positive cells in the resulting images of β-galactosidase staining, cellular immunofluorescence, and immunohistochemistry. Data were analyzed using GraphPad Prism version 9.4.1 (GraphPad Inc., USA). All data are reported as mean ± SE. The average difference between the 2 groups was analyzed by Student's *t*-test, and the statistical significance of multiple group comparisons was calculated by one-way analysis of variance (ANOVA). A P value < 0.05 was considered statistically significant.

Results

LIPUS directly inhibited DOX-induced chondrocyte senescence

The DOX-treated senescent RCS cells exhibited a high positive rate of SA-β-gal, which LIPUS significantly reduced (Figure 1A and B). Compared with the control group, the DOX-induced senescent chondrocytes had significantly increased expression of the senescence marker proteins p53, p21, and p16^{INK4a}, and decreased type II collagen and senescence marker protein lamin B1 expression, and increased MMP-13 expression. Treatment with LIPUS inhibited DOX-induced p53, p21, p16^{INK4a}, and MMP-13 expression, and increased type II collagen and lamin B1 expression (Figure 1C and D). The changes of p21 and DNA damage protein γh2ax in chondrocytes were detected using immunofluorescence. Consistent with previous results, LIPUS suppressed the DOX-induced expression of p21 and reduced γh2ax foci (Figure 2A and B). Oxidative stress and excessive ROS

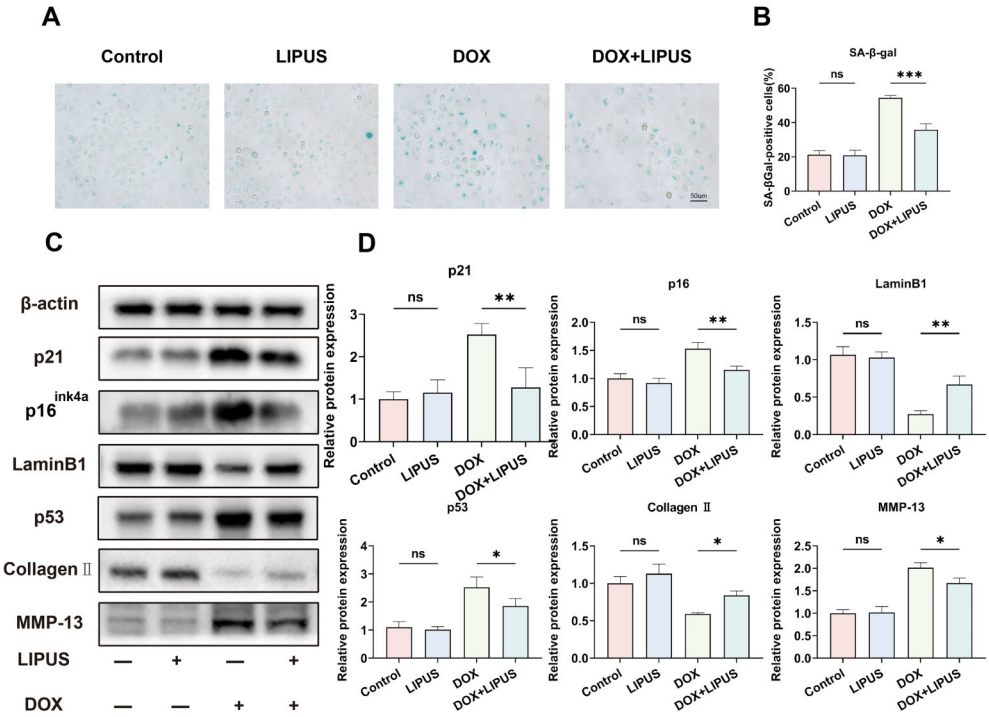

Figure 1. Low intensity pulsed ultrasound (LIPUS) directly inhibited the doxorubicin (DOX) induced chondrocyte senescence. **A** and **B**, SA-β-gal staining in chondrocytes, n=3. **C** and **D**, Protein expressions of p21, $p16^{INK4a}$, laminB1, p53, collagen II, and MMP-13 in chondrocytes shown by western blotting. Data are reported as mean and SE. *$P<0.05$, **$P<0.01$, ***$P<0.001$, ns: non-significant (ANOVA).

levels play negative roles in OA pathogenesis. DOX-mediated cellular senescence is driven by oxidative stress, which is also evidenced by elevated ROS levels (18). LIPUS directly reduced the production of ROS induced by DOX (Figure 2C and D). The results suggested that LIPUS attenuated DOX-induced chondrocyte senescence.

LIPUS inhibited SASP factors expression in DOX-induced senescent chondrocytes

SASP factors expression is increased in senescent chondrocytes. Elevated production of proinflammatory mediators, (interleukin (IL)-17, IL-6, CCL4, CCL2, CXCL1, and MMP-13) is the main feature of SASP, which is closely related to OA onset and progression (19). The results showed that LIPUS decreased the mRNA expression of two senescence markers, CDKN1a and CDKN2a (Figure 3A). We also found that LIPUS significantly reduced the DOX-induced IL-17, IL-6, CCL4, CCL2, and CXCL1 mRNA expression (Figure 3A). Furthermore, ELISA results showed that LIPUS also significantly inhibited CCL2, CXCL1, CCL4, and MMP-13 protein expression (Figure 3B). These findings demonstrated that LIPUS directly inhibited SASP factor secretion in DOX-induced senescent chondrocytes. To increase the reliability of the *in vitro* experimental results, we also extracted primary chondrocytes from c57 mice to verify the impact of LIPUS on chondrocyte senescence, and obtained consistent results (Figure 4).

LIPUS inhibited chondrocyte senescence and secretion of SASP factors CCL4 and CCL2 by regulating the PI3K/AKT/mTOR signaling pathway

PI3K/AKT/mTOR signaling is involved in the regulation of cellular senescence in various diseases (20). A previous study showed that inhibition of the PI3K/AKT/mTOR signaling pathway could attenuate chondrocyte senescence (21). The effect of LIPUS on PI3K/AKT/mTOR signaling in DOX-induced chondrocytes was detected by western blotting. We found that DOX increased p-PI3K, p-AKT, and p-mTOR expression compared with the control. Moreover, LIPUS significantly attenuated DOX-upregulated p-PI3K, p-AKT, and p-mTOR levels (Figure 5A). We examined whether LIPUS inhibits chondrocyte senescence by regulating the PI3K/AKT/mTOR signaling pathway by pre-treating chondrocytes with a PI3K inhibitor (LY294002) and agonist (740Y-P), and detected senescence-related proteins levels and SASP factors CCL4 and CCL2 secretion in chondrocytes by western blot and ELISA, respectively. Both LY294002

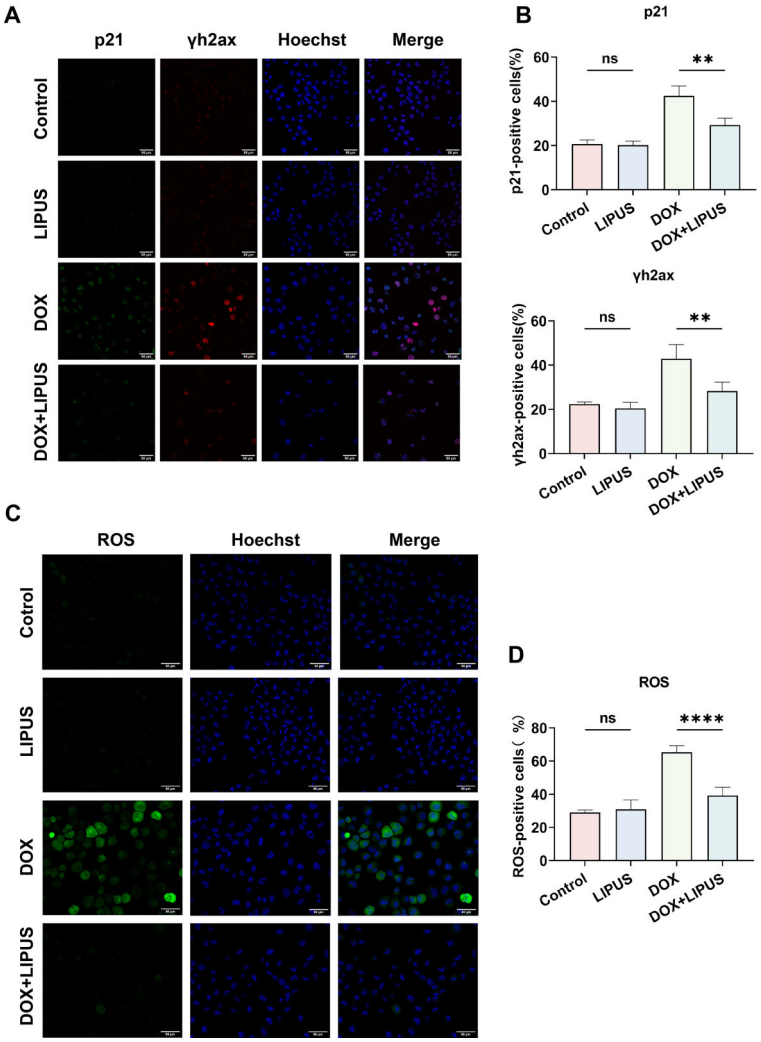

Figure 2. Low intensity pulsed ultrasound (LIPUS) directly inhibited the doxorubicin (DOX)-induced chondrocyte senescence and reactive oxygen species (ROS) production. **A** and **B**, Immunofluorescence for p21 and γh2ax. **C** and **D**, Intracellular ROS measured by DCFH-DA staining (Scale bar=50 μm). Data are reported as mean and SE. **P < 0.01, ****P < 0.0001, ns: non-significant (ANOVA).

and LIPUS decreased the expression of DOX-induced senescence markers p53, $p16^{INK4a}$, and p21 and SASP factors CCL4 and CCL2, and also increased the expression of lamin B1. There was no statistical difference between the groups. 740Y-P further increased senescence markers p53, $p16^{INK4a}$, and p21and SASP factors CCL4 and CCL2 expression, and also further reduced the expression of lamin B1. Moreover, the therapeutic effect of LIPUS was counteracted by 740Y-P (Figure 5B and C). In addition, we performed β-galactosidase staining to detect the senescent phenotype of chondrocytes and obtained consistent changes (Figure 5D). These findings suggested that LIPUS may exert its therapeutic effects through the inhibition of the PI3K/AKT/mTOR pathway.

LIPUS attenuated chondrocyte senescence and cartilage degeneration in DMM mice

The effect of LIPUS on OA cartilage was studied via the DMM mouse model (Figure 6A). Cartilage degeneration was evaluated using a specific staining and scoring system (22). Compared with the DMM group, LIPUS-treated mice had less cartilage loss and significantly lower OARSI scores (Figure 6B and D). Additionally, the expression of cartilage degeneration marker MMP-13, the senescence markers p53, p21, $p16^{INK4a}$, lamin B1, and type II collagen were evaluated with IHC. Compared with the control group, the DMM cartilage had p53, p21, $p16^{INK4a}$, and MMP-13 positive regions, and fewer type II collagen and lamin B1 positive regions. Compared to the

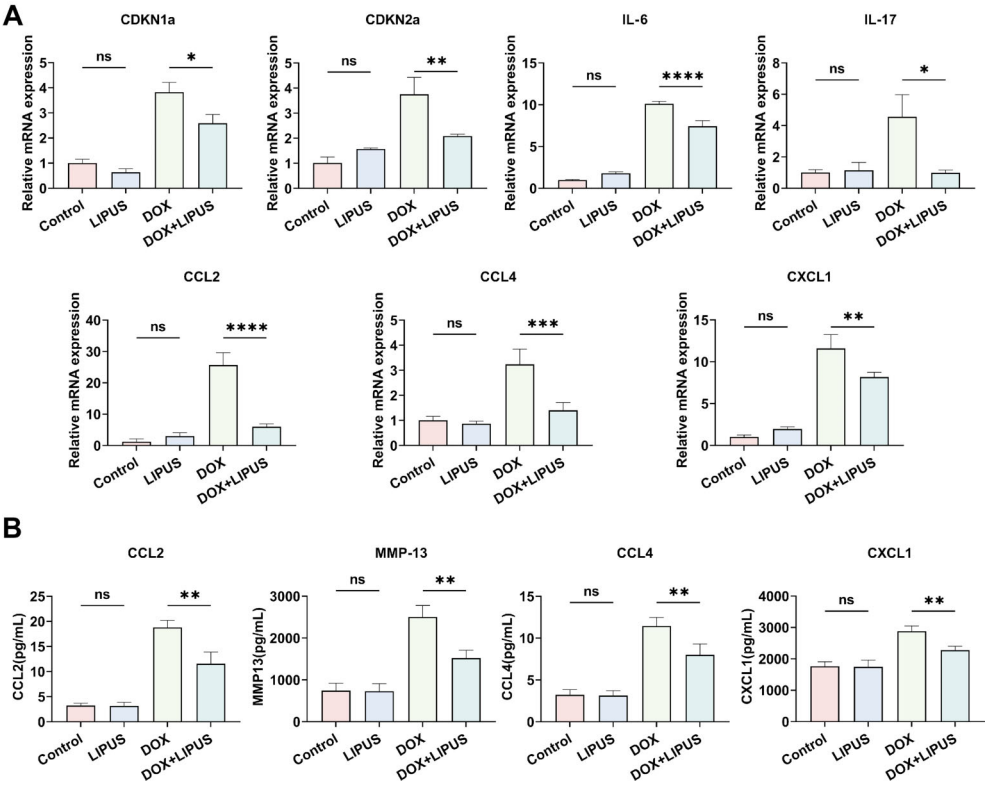

Figure 3. Low intensity pulsed ultrasound (LIPUS) directly inhibited the doxorubicin (DOX)-induced chondrocyte senescence-associated secretory phenotype. **A**, The mRNA expressions of CDKN1a, CDKN2a, interleukin (IL)-6, IL-17, CCL2, CCL4, and CXCL1 were detected by RT-qPCR. **B**, The levels of CCL2, MMP-13, CCL4, and CXCL1 in the cell supernatants were assayed by ELISA. Data are reported as mean and SE. *P < 0.05, **P < 0.01, ***P < 0.001, ****P < 0.0001, ns: non-significant (ANOVA).

DMM mice, LIPUS treatment decreased p53, p21, $p16^{INK4a}$, and MMP-13 expression, and increased type II collagen and lamin B1 expression in mouse cartilage (Figure 6B and C). Cartilage extracellular matrix (ECM) instability plays an important role in the pathogenesis of OA, and MMP-13 is an important regulatory factor (23). LIPUS treatment significantly reduced the MMP-13-positive region in articular cartilage of DMM mice, while also increasing type II collagen expression and reversing the subsequent degradation of articular cartilage matrix. The results suggested that LIPUS treatment alleviated chondrocyte senescence and cartilage deterioration in DMM-induced OA mice.

Discussion

Cellular senescence has always been an important cause of age-related diseases, and inhibiting senescence is a perpetual human pursuit (24). A growing number of studies have proven that chondrocyte senescence plays a crucial role in OA onset and progression (6). Moreover, clearing senescent chondrocytes attenuated OA progression and promoted cartilage homeostasis (25). In this study, we determined the role of LIPUS in attenuating chondrocyte senescence in OA.

Stimuli such as oxidative stress, chronic inflammation, and abnormal mechanical stress all contribute to chondrocyte senescence (26). Chondrocyte senescence affects cartilage homeostasis and normal cellular function (27). Senescent chondrocytes commonly exhibit elevated SA-β-gal levels, loss of lamin B1, and accumulated DNA damage (28). LIPUS significantly reduced the proportion of SA-β-gal-positive cells. In addition, both western blotting and immunohistochemistry results proved that LIPUS increased lamin B1 levels. Kirsch et al. (18) found that ROS levels significantly increased in DOX-induced senescent chondrocytes, which was related to oxidative stress. Our results have shown that LIPUS significantly reduced ROS production. Previous studies have confirmed that increased ROS level impairs the repair process of damaged DNA in chondrocytes (29). As shown by immunofluorescence analysis, LIPUS reduced the number of γ-h2ax foci present at DNA double-strand break sites in senescent chondrocytes.

The chondrocyte senescence process is triggered by increased expression of $p16^{INK4a}$/Rb and p53/p21CIP1

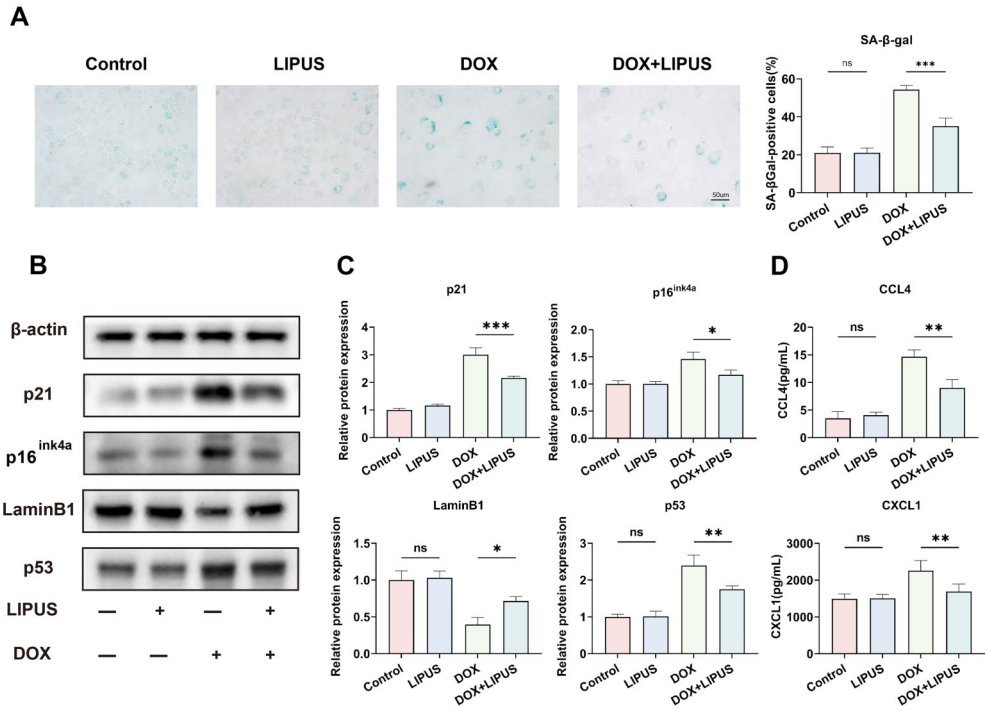

Figure 4. Low intensity pulsed ultrasound (LIPUS) inhibited doxorubicin (DOX)-induced senescence and expression of senescence-associated secretory phenotype factors CCL4 and CXCL1 in primary mouse chondrocytes. **A**, SA-β-gal staining in primary mouse chondrocytes; scale bar=50 μm. **B** and **C**, The protein expressions of p21, $p16^{INK4a}$, laminB1, and p53 in primary mouse chondrocytes shown in western blotting. **D**, The levels of CXCL1 and CCL4 in the primary mouse chondrocytes supernatants were assayed by ELISA. Data are reported as mean and SE. *P < 0.05, **P < 0.01, ***P < 0.001, ns: non-significant (ANOVA).

signaling, under various stresses (30). According to our results, LIPUS significantly downregulated the levels of senescence marker proteins p21, $p16^{INK4a}$, and p53 in chondrocytes *in vivo* and *in vitro*. SASP significantly contributes to OA progression.

SASP factors such as IL-17, IL-6, CCL4, CCL2, CXCL1, and MMP-13 released by senescent chondrocytes promote the development of OA by promoting an inflammatory environment within the joint, accelerating cartilage matrix degradation (8). In this study, we demonstrated for the first time that LIPUS inhibited the senescence phenotype of chondrocytes both *in vivo* and *in vitro*. What is more noteworthy is that LIPUS also downregulated the expression of SASP factors (IL-17, IL-6, CCL4, CCL2, CXCL1, and MMP-13) in senescent chondrocytes. Interestingly, CCL2 was found to recruit monocytes and macrophages to spread inflammation and tissue damage in OA (31). Another recent study demonstrated that M1 macrophage-derived IL-18 induces articular chondrocyte senescence (32). This suggests that LIPUS may affect macrophages through chondrocytes, which deserves further study.

DMM surgery reduced the intensity of safranin-O staining on the articular cartilage surface and increased the OARSI score. HE staining also indicated the roughening of the cartilage surface as well as the reduction and disordered arrangement of chondrocytes. We found that LIPUS reversed and alleviated these histological changes. ECM instability is crucial in OA pathogenesis, with MMP-13 serving as a key regulatory element in this process (23). LIPUS treatment significantly reduced MMP-13 levels in articular cartilage of DMM mice, while also increasing the type II collagen levels and reversing the subsequent degradation of articular cartilage matrix. In addition, the proportion of $p16^{INK4a}$, p21, and p53-positive chondrocytes in the LIPUS-treated mice decreased, and the proportion of lamin B1-positive cells increased. These data were consistent with *in vitro* results showing that LIPUS inhibited the chondrocyte senescence phenotype.

The PI3K/AKT/mTOR pathway is the main regulator of cell survival, proliferation, and metabolism (33). Previous studies reported that abnormal activation of the PI3K/AKT/mTOR pathway aggravates the inflammatory response of chondrocytes and promotes the degradation of cartilage extracellular matrix, which is directly related to cartilage degeneration (7). It is worth noting that abnormal activation of the PI3K/AKT/mTOR pathway is a critical factor in chondrocyte senescence (34). The sustained activation of PI3K/AKT/mTOR signaling inhibits the autophagy

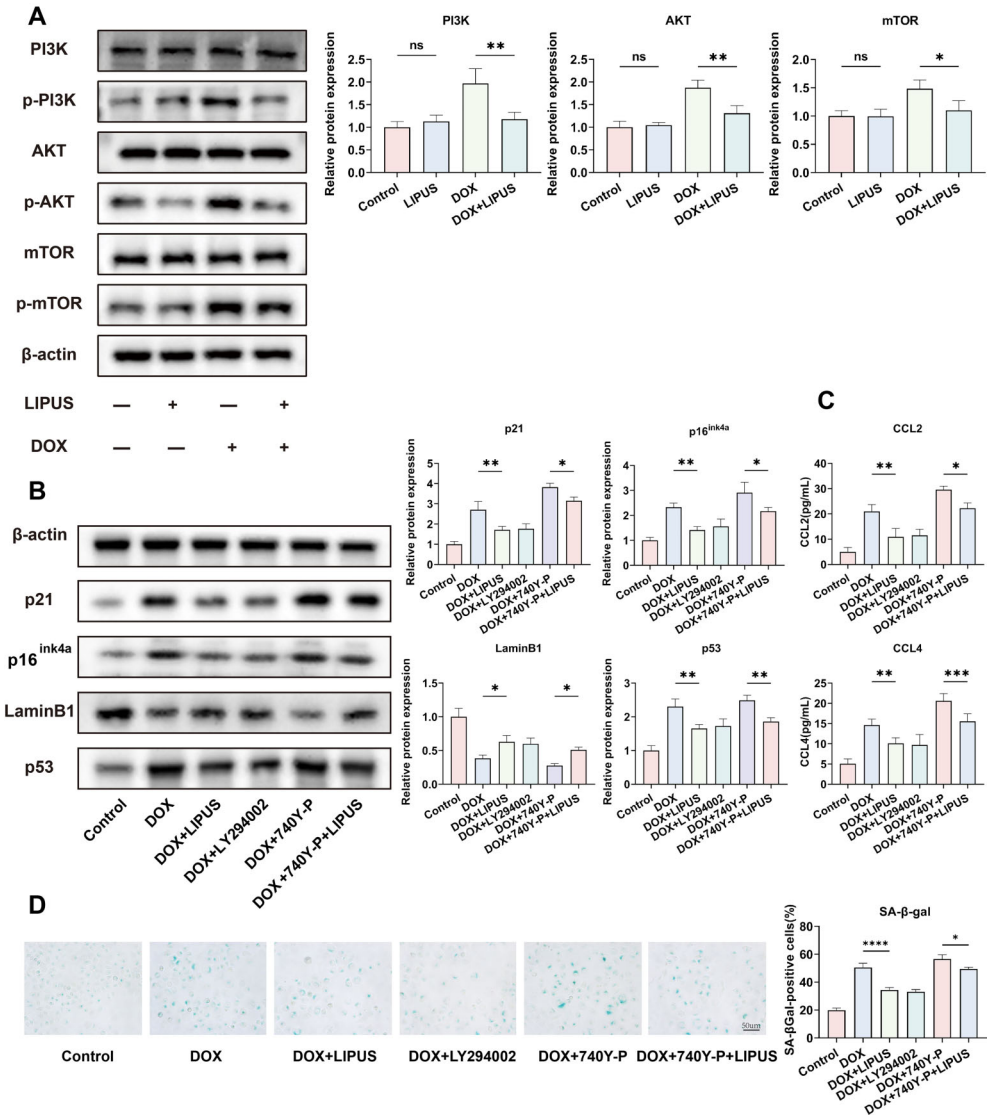

Figure 5. Low intensity pulsed ultrasound (LIPUS) inhibited chondrocyte senescence and the secretion of senescence-associated secretory phenotype factors CCL4 and CCL2 by regulating the PI3K/AKT/mTOR signaling pathway. **A**, Activation of phosphorylated PI3K/AKT/mTOR examined by western blot. **B**, The protein expressions of p21, $p16^{INK4a}$, laminB1 and p53 in chondrocytes pre-treated with LY294002 (50 μM) or 740Y-P (30 μM) shown in western blotting. **C**, The CCL4 and CCL2 levels in supernatants of chondrocytes pre-treated with LY294002 (50 μM) or 740Y-P (30 μM) were measured by ELISA. **D**, SA-β-gal staining in chondrocytes pre-treated with LY294002 (50 μM) or 740Y-P (30 μM), n=3; scale bar=50 μm. Data are reported as mean and SE. *$P<0.05$, **$P<0.01$, ***$P<0.001$, ****$P<0.0001$, ns: non-significant (ANOVA).

process, and aggravates the accumulation of damaged molecules in chondrocytes, thereby accelerating the senescence and degenerative changes of chondrocytes (35). In addition, activation of mTOR signaling is associated with increased oxidative stress and DNA damage, which will further exacerbate the senescent process of chondrocytes (36). In this study, we found that LIPUS significantly inhibited the abnormal activation of the PI3K/AKT/mTOR signaling pathway in DOX-induced senescent chondrocytes. In addition, inhibiting and activating the PI3K/AKT/mTOR signaling pathway can reverse and enhance the expression of key protein molecules in chondrocyte senescence. However, the PI3K agonist 740Y-P reversed the inhibitory effect of LIPUS on chondrocyte senescence by activating PI3K/AKT/mTOR. Our findings suggested that LIPUS attenuated chondrocyte senescence by inhibiting PI3K/AKT/mTOR signaling to maintain cartilage homeostasis during OA progression.

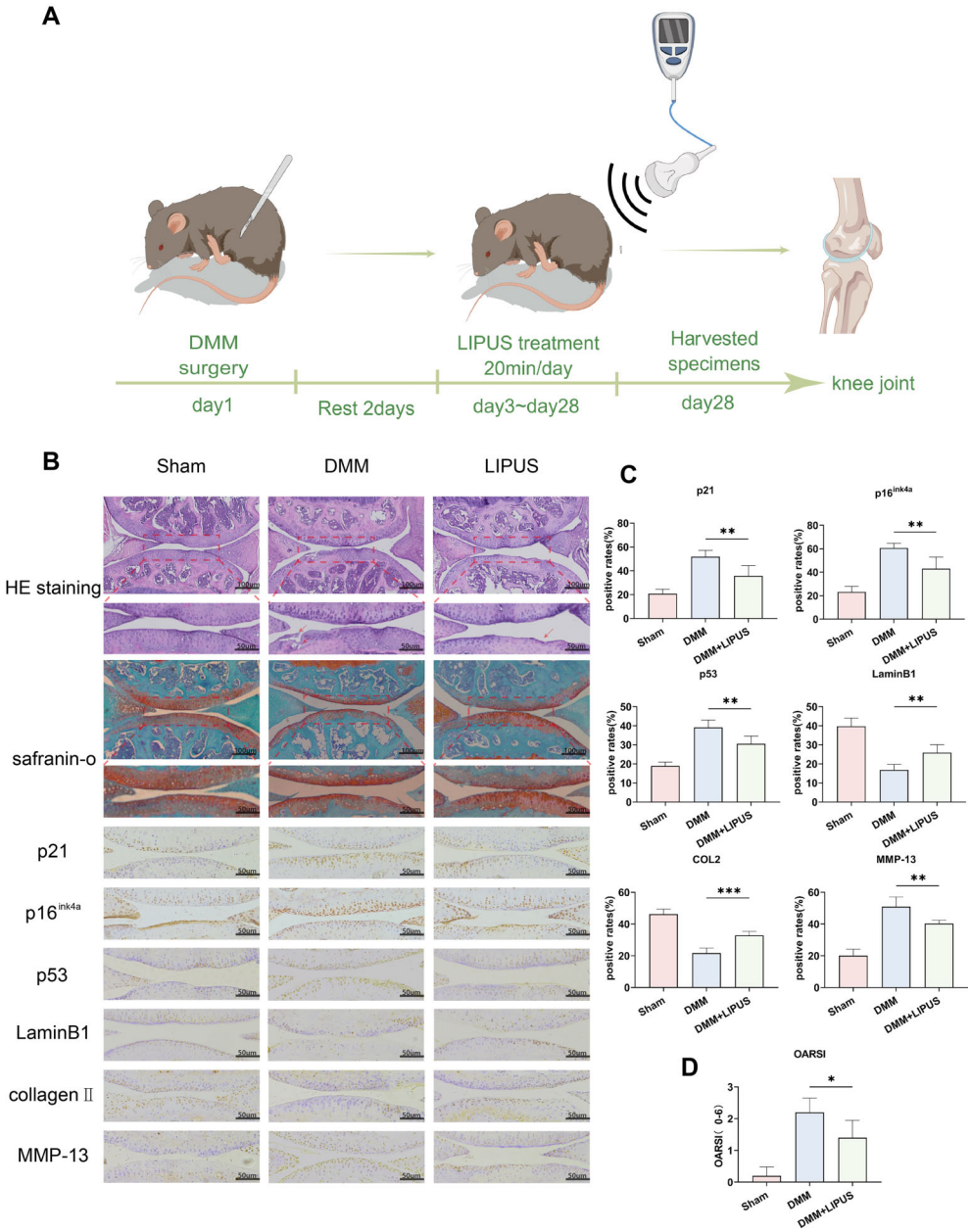

Figure 6. A, Animal experiment flow chart. Osteoarthritis was induced in mice by destabilization of the medial meniscal (DMM) surgery and were treated with low intensity pulsed ultrasound (LIPUS) (30 mW/cm^2) according to the process shown in the figure. **B** and **C**, Hematoxylin and eosin staining, safranin-O/fast green staining, and immunohistochemical staining for p21, p16^{INK4a}, p53, laminB1, collagen II, and MMP-13 of the cartilage. **D**, Osteoarthritis Research Society International (OASRI) score. Data are reported as mean and SE. *P < 0.05, **P < 0.01, ***P < 0.001, ns: non-significant (ANOVA). Scale bar, 50 μm.

Cellular senescence has been extensively explored in recent years. The emerging therapeutic strategies targeting senescent cells are senolytic and senomorphic (1). Senolytic therapy refers to drugs that specifically kill senescent cells, and senomorphic therapy refers to drugs that neutralize SASP and counteract its effects (37). UBX0101 selectively cleared senescent cells in the joints of post-traumatic OA mice and alleviated OA progression (8). Navitoclax (ABT-263) induced the apoptosis of senescent cells and attenuated articular cartilage degeneration in rats (38). Nevertheless, ABT-263 injection led to the worrisome adverse effect of severe thrombocytopenia (39). The delivery

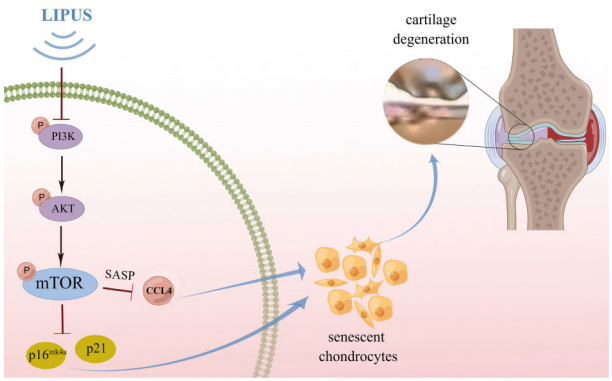

Figure 7. Schematic diagram. Low intensity pulsed ultrasound (LIPUS) inhibited chondrocyte senescence and senescence-associated secretory phenotype by regulating the PI3K/AKT/mTOR signaling pathway.

of rapamycin by PLGA microparticles significantly decreased SASP factors and alleviated the OA severity in DMM mice (40). The safety of these drugs, however, requires further study. It is worth noting that LIPUS is a non-invasive, safe, and widely used physical rehabilitation therapy. Our study is the first to systematically explore the role of LIPUS in inhibiting chondrocyte senescence. This finding expands our understanding of non-pharmacological interventions in joint diseases, particularly in addressing cellular senescence. Through our research on LIPUS, we offer new perspectives on potential non-invasive therapeutic approaches for chondrocyte senescence.

Conclusions

We determined that LIPUS inhibited chondrocyte senescence and SASP by regulating the PI3K/AKT/mTOR signaling pathway (Figure 7). Although LIPUS showed promising efficacy in our study, its clinical application still faces challenges. Firstly, treatment parameters such as frequency and intensity have not been standardized, and individual response variability may affect efficacy. Additionally, current research on the long-term safety of LIPUS is relatively limited, necessitating further clinical trials to assess its applicability across different patient populations. Therefore, future research must address these technical and biological challenges to ensure that LIPUS can be applied safely and effectively in the treatment of OA.

Supplementary Material

Click here to view [pdf].

Funding

This project was supported by the National Natural Science Foundation of China (grant numbers 82002402 and 82172533), the Natural Science Foundation of Chongqing (grant numbers CSTB2023NSCQ-MSX0361), and the Scientific and Technological Research Program of Chongqing Municipal Education Commission (grant numbers KJQN202300485).

References

1. Di Micco R, Krizhanovsky V, Baker D, d'Adda di Fagagna F. Cellular senescence in ageing: from mechanisms to therapeutic opportunities. Nat Rev Mol Cell Biol. 2021;22(2):75-95, doi: 10.1038/s41580-020-00314-w.
2. Huang W, Hickson LJ, Eirin A, Kirkland JL, Lerman LO. Cellular senescence: the good, the bad and the unknown. Nat Rev Nephrol. 2022;18(10):611-627, doi: 10.1038/s41581-022-00601-z.
3. Herranz N, Gil J. Mechanisms and functions of cellular senescence. J Clin Invest. 2018;128(4):1238-1246, doi: 10.1172/JCI95148.
4. Katz JN, Arant KR, Loeser RF. Diagnosis and treatment of hip and knee osteoarthritis: a review. JAMA. 2021;325(6):568-578, doi: 10.1001/jama.2020.22171.
5. Jeon OH, David N, Campisi J, Elisseeff JH. Senescent cells and osteoarthritis: a painful connection. J Clin Invest. 2018;128(4):1229-1237, doi: 10.1172/JCI95147.
6. Coryell PR, Diekman BO, Loeser RF. Mechanisms and therapeutic implications of cellular senescence in osteoarthritis. Nat Rev Rheumatol. 2021;17(1):47-57, doi: 10.1038/s41584-020-00533-7.
7. Sun K, Luo J, Guo J, Yao X, Jing X, Guo F. The PI3K/AKT/mTOR signaling pathway in osteoarthritis: a narrative review. Osteoarthritis Cartilage. 2020;28(4):400-409, doi: 10.1016/j.joca.2020.02.027.
8. Jeon OH, Kim C, Laberge RM, Demaria M, Rathod S, Vasserot AP, et al. Local clearance of senescent cells attenuates the development of post-traumatic osteoarthritis and creates a pro-regenerative environment. Nat Med. 2017; 23(6):775-781, doi: 10.1038/nm.4324.
9. Liu X, Zou D, Hu Y, He Y, Lu J. Research progress of low-intensity pulsed ultrasound in the repair of peripheral nerve injury. Tissue Eng Part B Rev. 2023;29(4):414-428, doi: 10.1089/ten.teb.2022.0194.
10. Han S, Luo J, Xu S, Zhao L, Yao C, Xu J, et al. Low-intensity pulsed ultrasound alleviates human testicular leydig cell senescence *in vitro*. Int J Mol Sci. 2022;24(1):418, doi: 10.3390/ijms24010418.
11. Lin CY, Wang CC, Loh JZ, Chiang TC, Weng TI, Chan DC, et al. Therapeutic ultrasound halts progression of chronic kidney disease *in vivo* via the regulation of markers associated with renal epithelial-mesenchymal transition and senescence. Int J Mol Sci. 2022;23(21):13387, doi: 10.3390/ijms232113387.
12. Zhou W, Chen A, Ye Y, Ren Y, Lu J, Xuan F, et al. LIPUS combined with TFSC alleviates premature ovarian failure

by promoting autophagy and inhibiting apoptosis. Gynecol Endocrinol. 2023;39(1):2258422, doi: 10.1080/09513590.2023.2258422.
13. Zeng Q, Hong S, Wang X, Cheng Y, Sun J, Xia W. Regulation of exosomes secretion by low-intensity pulsed ultrasound in lung cancer cells. Exp Cell Res. 2019;383(1):111448, doi: 10.1016/j.yexcr.2019.05.029.
14. Guan M, Zhu Y, Liao B, Tan Q, Qi H, Zhang B, et al. Low-intensity pulsed ultrasound inhibits VEGFA expression in chondrocytes and protects against cartilage degeneration in experimental osteoarthritis. FEBS Open Bio. 2020;10(3):434-443, doi: 10.1002/2211-5463.12801.
15. Liao B, Guan M, Tan Q, Wang G, e Zhang R, Huang J, et al. Low-intensity pulsed ultrasound inhibits fibroblast-like synoviocyte proliferation and reduces synovial fibrosis by regulating Wnt/β-catenin signaling. J Orthop Translat. 2021;30:41-50, doi: 10.1016/j.jot.2021.08.002.
16. Zhang B, Chen H, Ouyang J, Xie Y, Chen L, Tan Q, et al. SQSTM1-dependent autophagic degradation of PKM2 inhibits the production of mature IL1B/IL-1β and contributes to LIPUS-mediated anti-inflammatory effect. Autophagy. 2020;16(7):1262-1278, doi: 10.1080/15548627.2019.1664705.
17. Pritzker KPH, Gay S, Jimenez SA, Ostergaard K, Pelletier JP, Revell PA, et al. Osteoarthritis cartilage histopathology: grading and staging. Osteoarthritis Cartilage. 2006;14(1):13-29, doi: 10.1016/j.joca.2005.07.014.
18. Kirsch V, Ramge JM, Schoppa A, Ignatius A, Riegger J. *In vitro* characterization of doxorubicin-mediated stress-induced premature senescence in human chondrocytes. Cells. 2022;11(7):1106, doi: 10.3390/cells11071106.
19. Liu Y, Zhang Z, Li T, Xu H, Zhang H. Senescence in osteoarthritis: from mechanism to potential treatment. Arthritis Res Ther. 2022;24(1):174, doi: 10.1186/s13075-022-02859-x.
20. Tang Q, Markby GR, MacNair AJ, Tang K, Tkacz M, Parys M, et al. TGF-β-induced PI3K/AKT/mTOR pathway controls myofibroblast differentiation and secretory phenotype of valvular interstitial cells through the modulation of cellular senescence in a naturally occurring *in vitro* canine model of myxomatous mitral valve disease. Cell Prolif. 2023;56(6):e13435, doi: 10.1111/cpr.13435.
21. Zhang Y, Cai W, Han G, Zhou S, LI J, Chen M, et al. Panax notoginseng saponins prevent senescence and inhibit apoptosis by regulating the PI3K-AKT-mTOR pathway in osteoarthritic chondrocytes. Int J Mol Med. 2020;45(4):1225-1236, doi: 10.3892/ijmm.2020.4491.
22. Glasson SS, Chambers MG, Van Den Berg WB, Little CB. The OARSI histopathology initiative - recommendations for histological assessments of osteoarthritis in the mouse. Osteoarthritis Cartilage. 2010;18 Suppl 3:S17-S23, doi: 10.1016/j.joca.2010.05.025.
23. Hu Q, Ecker M. Overview of MMP-13 as a promising target for the treatment of osteoarthritis. Int J Mol Sci. 2021;22(4):1742, doi: 10.3390/ijms22041742.
24. Chaib S, Tchkonia T, Kirkland JL. Cellular senescence and senolytics: the path to the clinic. Nat Med. 2022;28(8):1556-1568, doi: 10.1038/s41591-022-01923-y.
25. Yang H, Chen C, Chen H, Duan X, Li J, Zhou Y, et al. Navitoclax (ABT263) reduces inflammation and promotes chondrogenic phenotype by clearing senescent osteoarthritic chondrocytes in osteoarthritis. Aging (Albany NY). 2020;12(13):12750-12770, doi: 10.18632/aging.103177.
26. Khosla S, Farr JN, Monroe DG. Cellular senescence and the skeleton: pathophysiology and therapeutic implications. J Clin Invest. 2022;132(3):e154888, doi: 10.1172/JCI154888.
27. Boulestreau J, Maumus M, Jorgensen C, Noël D. Extracellular vesicles from mesenchymal stromal cells: therapeutic perspectives for targeting senescence in osteoarthritis. Adv Drug Deliv Rev. 2021;175:113836, doi: 10.1016/j.addr.2021.113836.
28. Varghese SS, Dhawan S. Senescence: a double-edged sword in beta-cell health and failure? Front Endocrinol (Lausanne). 2023;14:1196460, doi: 10.3389/fendo.2023.1196460.
29. Reed KN, Wilson G, Pearsall A, Grishko VI. The role of mitochondrial reactive oxygen species in cartilage matrix destruction. Mol Cell Biochem. 2014;397(1-2):195-201, doi: 10.1007/s11010-014-2187-z.
30. Wan M, Gray-Gaillard EF, Elisseeff JH. Cellular senescence in musculoskeletal homeostasis, diseases, and regeneration. Bone Res. 2021; 9(1):41, doi: 10.1038/s41413-021-00164-y.
31. Raghu H, Lepus CM, Wang Q, Wong HH, Lingampalli N, Oliviero F, et al. CCL2/CCR2, but not CCL5/CCR5, mediates monocyte recruitment, inflammation and cartilage destruction in osteoarthritis. Ann Rheum Dis. 2017;76(5):914-922, doi: 10.1136/annrheumdis-2016-210426.
32. Dong L, Zhao Y, Sun C, Yang ZO, Chen F, Hu W, et al. ASIC1a-CMPK2-mediated M1 macrophage polarization exacerbates chondrocyte senescence in osteoarthritis through IL-18. Int Immunopharmacol. 2023;124(Pt A):110878, doi: 10.1016/j.intimp.2023.110878.
33. Manning BD, Toker A. AKT/PKB signaling: navigating the network. Cell. 2017;169(3):381-405, doi: 10.1016/j.cell.2017.04.001.
34. He X, Hu W, Zhang Y, Chen M, Ding M, Yang H, et al. Cellular senescence in skeletal disease: mechanisms and treatment. Cell Mol Biol Lett. 2023;28(1):88, doi: 10.1186/s11658-023-00501-5.
35. Lotz MK, Caramés B. Autophagy and cartilage homeostasis mechanisms in joint health, aging and OA. Nat Rev Rheumatol. 2011;7(10):579-587, doi: 10.1038/nrrheum.2011.109.
36. Lee Y, Kim J, Kim MS, Kwon Y, Shin S, Yi H, et al. Coordinate regulation of the senescent state by selective autophagy. Dev Cell. 2021;56(10):1512-1525.e7, doi: 10.1016/j.devcel.2021.04.008.
37. Guo J, Huang X, Dou L, Yan M, Shen T, Tang W, et al. Aging and aging-related diseases: from molecular mechanisms to interventions and treatments. Signal Transduct Target Ther. 2022;7(1):391, doi: 10.1038/s41392-022-01251-0.
38. Miura Y, Endo K, Komori K, Sekiya I. Clearance of senescent cells with ABT-263 improves biological functions of synovial mesenchymal stem cells from osteoarthritis patients. Stem Cell Res Ther. 2022;13(1):222, doi: 10.1186/s13287-022-02901-4.
39. Khan S, Zhang X, Lv D, Zhang Q, He Y, Zhang P, et al. A selective BCL-XL PROTAC degrader achieves safe and potent antitumor activity. Nat Med. 2019;25(12):1938-1947, doi: 10.1038/s41591-019-0668-z.
40. Dhanabalan KM, Dravid AA, Agarwal S, Sharath RK, Padmanabhan AK, Agarwal R. Intra-articular injection of rapamycin microparticles prevent senescence and effectively treat osteoarthritis. Bioeng Transl Med. 2023;8(1):e10298, doi: 10.1002/btm2.10298.